

Formation of the G-ring arc

N. C. S. Araujo^{1*}; E. Vieira Neto^{1†} and D. W. Foryta^{2‡}

¹ Departamento de Matemática, Univ. Estadual Paulista, 12516-410 Guaratinguetá, São Paulo, Brazil

² Departamento de Física, Univ. Federal do Paraná, 83531-940 Curitiba, Paraná, Brazil

Original form 2014 December 15; last revision 02 May 2016

ABSTRACT

Since 2004, the images obtained by Cassini spacecraft’s on-board cameras have revealed the existence of several small satellites in the Saturn system. Some of these small satellites are embedded in arcs of particles. While these satellites and their arcs are known to be in corotation resonances with Mimas, their origin remains unknown. This work investigates one possible process for capturing bodies into a corotation resonance, which involves raising the eccentricity of a perturbing body. Therefore, through numerical simulations and analytical studies, we show a scenario that the excitation of Mimas’ eccentricity could capture particles in a corotation resonance and given a possible explanation for the origin for the arcs.

Key words: planets and satellites: dynamical evolution – planets and satellites: rings – planets and satellites: individual (Mimas, Enceladus)

1 INTRODUCTION

Since 2004, the Cassini spacecraft has returned to Earth a copious amount of data about the Saturnian system. In particular, its imaging system revealed the existence of several small satellites. There are papers (Spitale et al. 2006; Cooper et al. 2008; Hedman et al. 2010) showing that Mimas perturbs the orbits of some of these satellites by resonant interactions.

In 2006 data returned by Cassini revealed an arc of dust inside the G-ring. Since then, this region has been explored by Hedman et al. (2007) precisely calculated the G arc’s mean motion using the Cassini’s data. It revealed that this arc is in a 7:6 corotation resonance with Mimas. Through the analysis of images obtained between 2008 and 2009, it was found that the satellite Aegaeon was located inside this arc (Hedman et al. 2010). And since this satellite is immersed in this arc, it is also trapped in this corotation resonance with Mimas.

Hedman et al. (2010) confirm this corotation resonance through numerical simulations of the full equations of motion. They also identify that this satellite is in corotation resonance with characteristic angle

$$\varphi_{CER} = 7\lambda_{Mimas} - 6\lambda_{Aegaeon} - \varpi_{Mimas}. \quad (1)$$

Their simulations also show that a nearby Lindblad res-

onance also influences the moon’s motion (Hedman et al. 2010).

Prior this study and also from Cassini images two others satellites were discovered, Methone in 2004 (Spitale et al. 2006) and Anthe in 2007 (Cooper et al. 2008). The numerical analysis of the full equations of motion (Spitale et al. 2006; Cooper et al. 2008) indicates that these satellites are in corotation resonances whose characteristic angles are, respectively,

$$\varphi_{CER} = 15\lambda_{Methone} - 14\lambda_{Mimas} - \varpi_{Mimas}, \quad (2)$$

$$\varphi_{CER} = 11\lambda_{Anthe} - 10\lambda_{Mimas} - \varpi_{Mimas}. \quad (3)$$

The Cassini images also show that Aegaeon, Anthe and Methone are immersed in tenuous arcs of particles (Hedman et al. 2007, 2009) and Hedman et al. (2010) said that these particles probably have been originated from the material knocked off, at low speeds, from the surface of these satellites. Therefore, these particles don’t have enough energy to escape the corotation resonance and then remain close to the satellite filling the nearby space. With these evidences Hedman et al. (2010) concluded that the study of these satellites and their arcs may improve the understanding of the connection between satellites and rings. Because these objects and their arcs are in corotation resonances, these satellites may be seen as a distinct class of objects in the Saturn system.

The existence of these satellites immersed in arcs of dust allows us to infer two possibilities for their origin. (i) The satellites were build-up by particles previously caught in resonance and their arcs are the vestiges of this formation. Alternatively, (ii) Mimas had captured satellites al-

* E-mail: nilcasr@gmail.com (NCSA)

† E-mail: ernesto@feg.unesp.br (EVN)

‡ E-mail: foryta@fisica.ufpr.br (DWF)

ready formed, and consequently the arcs had originated from particles that had broken off from these satellites.

Although we are not able to judge immediately which of the above statements are the correct one, we realize that both statements depend on the possibility of bodies been captured in corotation resonance with Mimas, either small particles or a full satellite. Thus, in this work we investigate the mechanism of capturing particles in corotation resonance.

The corotation resonance exists only when the perturbing satellite has eccentricity different from zero (Murray & Dermott 1999). Then, in our problem, corotation depends on the eccentricity of Mimas. And it is known that, due to tidal effects, the eccentricity of Mimas should be lower than the current value (Meyer & Wisdom 2008). But Mimas has a higher eccentricity than most of Saturn's regular satellites, it is likely that his eccentricity was increased through a resonant interaction with another satellite. In this work we will consider the presence of Enceladus playing an important role in this scenario.

The aim of this paper is to investigate the mechanisms which would make Mimas capture particles in a corotation resonance in the past of the Saturn system. The study will be made through numerical simulations and analytical studies which will be developed using the dynamics of three and four bodies problems considering the effects of non-spherical shape of Saturn.

In our problem the main bodies are Saturn, Mimas, Enceladus and particles of G-ring. We will study the scenario where particles will be captured in corotation resonance with Mimas when Mimas passes through a resonance with Enceladus. As a result of this study, we will have a better understanding of the dynamics involved in the origin and stability of small satellites. In this study, we will focus on 7:6 corotation resonance

In section 2 we make a brief discussion on the corotation resonance. Section 3 introduces the mechanism we develop to obtain the eccentricity variation of Mimas. Section 4 shows the effects of this mechanism on Mimas orbit. Section 5 presents the results of this mechanism when a ring of particles is immersed in the 7:6 corotation resonance region. In Section 6 we analyze the process of capture due the migration. Finally, the concluding remarks for this study will be found in the section 7.

2 RESONANCES IN OBLATE PLANETS

When an object orbits an oblate planet, its orbit experiences effects of a potential which depends on the planet's zonal harmonic coefficients J_2, J_4, \dots . The perturbations of that potential cause the rotation of the orbit in space, the precession of the unperturbed orbit.

The rotation of the orbit generates three frequencies: n , the mean motion; κ and ν , radial/vertical epicyclic frequency, respectively (Murray & Dermott 1999). Thereby, considering the additional gravitational effects of a perturbing satellite on a particle, when this system is around an oblate planet, the orbit of the particle can be analysed through those frequencies.

Those frequencies are associated with the precession of the node and pericenter of the orbit by $\kappa = n - \dot{\omega}$ and

$\nu = n - \dot{\Omega}$ and then the definition of the corotation resonance (Murray & Dermott 1999) occurs when:

$$\varphi_{CR} = j\lambda' + (k + p - j)\lambda - k\varpi' - p\Omega', \quad (4)$$

where the primed orbital elements belong to the perturbing satellite while the non-primed orbital elements belong to the particle, j, k, p are integer values.

When a particle is in corotation resonance with a perturbing satellite, some orbital parameters are modified. There are analytical models able to estimate the extent of these variations, for example, the Pendulum Model or the Hamiltonian Approach (Murray & Dermott 1999). The orbital parameters that is most strongly affected by a corotation resonance is the semi-major axis. Using the Pendulum Model, we can calculate the maximum width libration of the semi-major axis for corotation resonance.

The maximum width for a corotation resonance is (Murray & Dermott (1999), Eq. (10.10))

$$W_{CR} = 8 \left(\frac{a|R|}{3Gm_p} \right)^{1/2} a, \quad (5)$$

where a is the semi-major axis of the perturbed body, m_p is the central body's mass and R is the relevant term of the perturbing function, whose equation is

$$R = \frac{Gm'}{a'} f_d(\alpha) e'^{|k|} s'^{|p|} \cos \varphi_{CER}, \quad (6)$$

where the primed parameters are of the perturbing satellite, with m', a', e' and s' as the mass, semi-major axis, eccentricity and a value associated to the inclination I' , i.e. $s' = \sin(I'/2)$, $f_d(\alpha)$ is a function in Laplace's coefficients for the direct terms of the perturbing function, φ_{CER} is the corotation resonant angle, k and p are integers.

Therefore, from the above equations, we expect that to existence of the corotation resonance, the perturbing satellite's eccentricity must be different from zero.

3 MODEL

The current eccentricity of Mimas is approximately 0.02, and Meyer & Wisdom (2008) pointed out that this value is relatively high and would imply a much higher value in the past, or it was recently excited. It is known that the eccentricity of a satellite can be excited due to resonances (Murray & Dermott 1999), but the recent value of Mimas' eccentricity cannot be explained by present resonances such as Mimas-Tethys 4:2 mean motion resonance (Champanois & Vienne 1999; Callegari & Yokoyama 2010). Thus we suppose that Mimas experienced some event in the past that increased its eccentricity.

Meyer & Wisdom (2008) suggested that Mimas was captured by Enceladus or by Dione into a resonance while the eccentricity of Mimas was less than the current value. They verified that when Mimas came into some eccentricity-type resonance with one of these satellites, Mimas' eccentricity increased and even exceed its current value. After these satellites escaped from this resonance interaction, the tidal orbital evolution decreased their eccentricity to the current values, as we can notice in Figures 6, 7 and 9 from the paper of Meyer & Wisdom (2008). Therefore, these kind of resonant encounters could have temporarily increased Mimas'

eccentricity, which have flavoured the capture of particles in Mimas' corotation resonances.

In our study we adopt a scenario where we have Mimas-Enceladus 3:2 e-Mimas resonance¹ as discussed in Meyer & Wisdom (2008). That resonance would induce an increase in Mimas' eccentricity even larger than the current one, and after a certain time those satellites could go out of that resonance. After the escape, due to the tidal effects, the eccentricity of Mimas would decay to the current value (Meyer & Wisdom 2008).

In our scenario Mimas and Enceladus were closer to Saturn than they are today. Thus, we had to calculate a consistent position for them based on a satellite tidal evolution. For this task, we perform the procedures discussed below.

First, we evaluate the ratio of the semi-major axes α when Mimas and Enceladus were trapped in the 3:2 eccentricity mean motion resonance. When two satellites are in mean motion resonance, α remains approximately constant and can be calculated with (Champanois & Vienne 1999)

$$\alpha = \left(\frac{p+q}{p}\right)^{-2/3} \left(1 + \frac{q_1 \dot{\varpi}_M + q_2 \dot{\varpi}_E + q_3 \dot{\Omega}_M + q_4 \dot{\Omega}_E}{n_E(p+q)}\right)^{-2/3}, \quad (7)$$

where p , q , q_1 , q_2 , q_3 and q_4 are integers; while $\dot{\varpi}_M$, $\dot{\varpi}_E$, $\dot{\Omega}_M$ and $\dot{\Omega}_E$ are precession rates of longitude of pericenter, longitude of ascending node for Mimas and Enceladus, respectively, and n_E is the mean motion of Enceladus. Using the angles values for the 3:2 eccentricity mean motion resonance in equation (7), we get the ratio between the semi-major axes of Mimas and Enceladus when they were trapped in that resonance (Champanois & Vienne 1999). In this paper, the values of $\dot{\varpi}_M$, $\dot{\varpi}_E$, $\dot{\Omega}_M$ and $\dot{\Omega}_E$ are consistent with the geometric orbital elements (Renner & Sicardy 2006). For the case of our resonance, we find the values of q_1 , q_2 , q_3 and q_4 from the comparison between general resonant angle,

$$\varphi = p\lambda - (p+q)\lambda' + q_1\varpi + q_2\varpi' + q_3\Omega + q_4\Omega', \quad (8)$$

where λ , ϖ , and Ω are the mean longitude, longitude of pericenter and longitude of the ascending node, respectively for the inner satellite, while those longitudes with prime represent the angles for the outer satellite, with resonant angle as,

$$\varphi_e = 2\lambda_M - 3\lambda_E + \varpi_M, \quad (9)$$

where λ_M is the mean longitude of Mimas, λ_E is the mean longitude of Enceladus. After our evaluations, we obtain α equal to 0.7637895.

The next step was to find the semi-major axis of the satellites corresponding to our α . We will call those semi-major axis "ancient semi-major axes" and it can be evaluated through the equation (the development of the following equation can be seen at appendix A)

$$a_{0M} = \left[\frac{a_M^{13/2} \left(\frac{m_E}{m_M}\right) - a_E^{13/2}}{\left(\frac{m_E}{m_M}\right) - \frac{1}{\alpha^{13/2}}} \right]^{2/13}, \quad (10)$$

where a_{0M} is the Mimas' ancient semi-major axis, a_M , a_E ,

¹ e-Mimas resonance is the notation of Meyer & Wisdom (2008) for Mimas' eccentricity-type first order resonance.

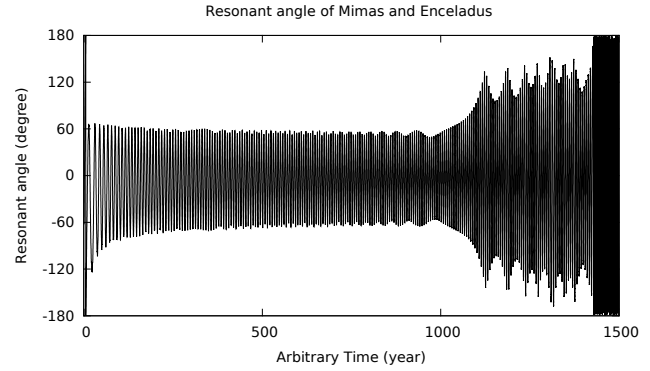


Figure 1. Critical angle for Mimas-Enceladus 3:2 e-Mimas resonance (equation (9)) during the migration process. It shows a libration around zero. To the end of tandem migration the critical angle increases its sweep following the increase on the eccentricity of Mimas.

m_M and m_E are the current semi-major axes and mass of the satellites Mimas and Enceladus, respectively.

Equation (10) is a function of α , the Mimas and Enceladus' semi-major axes ratio. As we had used a value of α when both satellites were in resonance with each other, we can locate the ancient semi-major axis of Enceladus using $a_{0E} = a_{0M}/\alpha$. The results of a_{0E} and a_{0M} indicate that those satellites were more distant from each other in the past compared with their current positions. As expected, since the inner satellite migrate faster than the outer one.

The values of Mimas and Enceladus ancient semi-major axis, calculated through equation (10), are approximated values. To obtain values which lead the system to enter in the resonance we try some values near the ancient semi-major axes until we got them close to a position in the verge of resonance.

The tidal effect can cause Saturn's satellites migration with velocity orders between of 10^{-7} and 10^{-5} km per year at their current positions (Meyer & Wisdom 2008; Lainey et al. 2012). Therefore, we should migrate Mimas and Enceladus with velocities close to those velocities. However, if we did that, it would take a long computational time, as we have noted in migration tests using that order of magnitude for the migration rate. As we are trying to prove the concept of corotation eccentricity resonance capture caused by the eccentricity of Mimas when it was enlarged due to mean motion resonance with Enceladus, therefore we used values which make our simulations more quickly. Thus, we migrate Mimas with a rate for the semi-major axis close to 1 km per year and Enceladus around 0.01 km per year. The external satellite will migrate slower than the internal one (see equation (A3) and also Burns & Matthews 1986). To generate those rates, we inserted into the dynamic of each satellite a drag force

$$\vec{F}_p = -\gamma v \vec{v}, \quad (11)$$

where \vec{v} is the velocity of the satellite, and γ a constant which will give the mentioned velocities for the semi-major axis. The value of semi-major axis will increase due to a negative sign for γ .

In a scenario with a lower eccentricity value for Enceladus, using the three-bodies dynamics for Saturn, Mi-

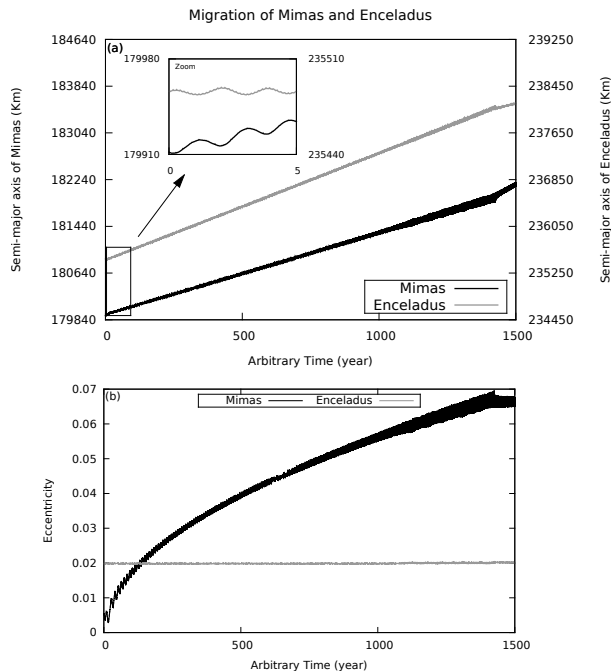


Figure 2. When Mimas is caught in resonance by Enceladus its eccentricity grows as seen in the lower panel. During this time a tandem migration is established resulting in a net migration rate, that differs from the tidal evolution alone, as seen in upper plot. The net migration rate of Enceladus raises by the interaction with Mimas while Mimas' migration rate decreases. This effect ends after the escape of the resonance and the migration rates change, as can be seen in the end of the figure (a).

mas and Enceladus, we found no chaotic behaviour for the resonance angle when we have Mimas-Enceladus 3:2 e-Mimas resonance. That is, we have found the same results that Meyer & Wisdom (2008) had encountered for Mimas-Enceladus 3:2 e-Enceladus resonance. It means that Mimas does not escape from the resonance capture during our time integration. This integration had run for 3000 years of arbitrary time (equivalent approximately to 300 million years, if we have used the correct rates for migration).

Tidal effects could have reduced a higher eccentricity of Enceladus, and in our scenario we verified that this higher eccentricity is necessary for Mimas to escape from the resonance. Higher values for Enceladus' eccentricity are possible due to earlier captures into others resonances as can be seen in Meyer & Wisdom (2007).

We used respectively 0.005 and 0.02 for the initial eccentricities of Mimas and Enceladus. These values make our scenario works very well as we will show below. Probably they may exist other mechanisms which could take Mimas out of the resonance other than this value for the eccentricity of Enceladus, but we are most interested in proving that the corotation resonance is able to capture particles, and we will investigate those features in other works.

4 MIGRATION EFFECTS ON MIMAS ORBIT

In the first part of our hypotheses, we treat the excitation on Mimas eccentricity due to its passage through the

Table 1. Initial Conditions of Enceladus and Mimas in Orbital Elements, after changes commented in Section 3.

Name	Mimas
Mass	3.75×10^{22} g
Radius	198.8 km
a	1.799177×10^5 km
e	5.0×10^{-3}
I	1.563 223 deg
Ω	3.564454×10^2 deg
ϖ	1.899002×10^2 deg
λ	3.166168×10^2 deg
Name	Enceladus
Mass	10.805×10^{22} g
Radius	252.3 km
a	2.354949×10^5 km
e	2.0×10^{-2}
I	5.067876×10^{-3} deg
Ω	2.633612×10^2 deg
ϖ	2.822281×10^2 deg
λ	2.950096×10^2 deg

Mimas-Enceladus 3:2 e-Mimas resonance during the migration process of these satellites. To perform this simulation we used the Gauss-Radau spacings described by Everhart (1985) with initial time step of 0.1 day. The dynamics of this process included Mimas, Enceladus and an oblate Saturn, and also the drag force of equation (11). For the initial conditions of Mimas and Enceladus, we use the consideration commented in Section 3 to form the set of initial condition shown in table 1.

In Figure (1) we observe the behaviour of the critical angle for Mimas-Enceladus 3:2 e-Mimas resonance (equation (9)). This behaviour occurs due to the passage of Mimas and Enceladus through the resonance during the migration process. We can see that at the very beginning of the simulation the Mimas-Enceladus system was not in resonance (the resonant angle circulates) and, due to the system migration, those satellites enter in the Mimas-Enceladus 3:2 e-Mimas resonance (Meyer & Wisdom 2008) in which the resonant angle librates around 0° . We can see along the migration process a decreasing amplitude for the resonant angle, it may turn the resonance between them more robust. Subsequently, this amplitude begins to increase until it reaches the value of 180° . At this point, we can say that Mimas and Enceladus are out of the resonance.

In Figure (2a) we can see the behaviour of Mimas' and Enceladus' semi-major axes during the migration process. Before they enter in resonance, the variation rates for the semi-major axis are the ones stated in the last section, with Enceladus migrating slower than Mimas (see zoom in Figure (2a)). After they enter in resonance, the rate of Enceladus' semi-major axis variation increases until reaching a value slightly larger than Mimas, while the semi-major axis rate variation for Mimas decreases. These can be seen in the semi-major axis inclination showed in Figure (2a). When they come out of resonance, the variation rates for the semi-major axis returns to their previous values.

This passage through the resonance affects Mimas' eccentricity significantly, as shown in Figure (2b). When Mimas is in resonance, its eccentricity increases to high values while Enceladus eccentricity remains constant. Despite the migration velocity, we have adopted, the behaviour for Mi-

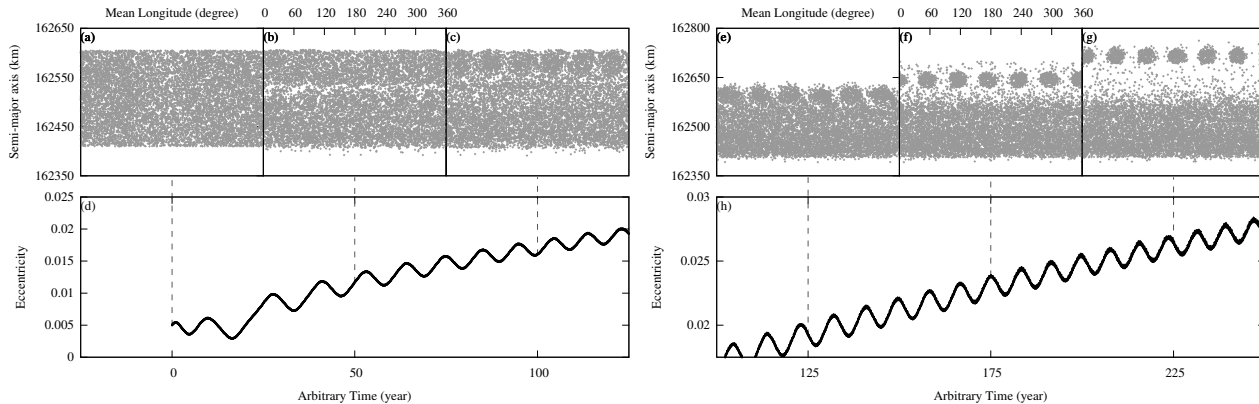


Figure 3. These six snapshots show the evolution of the capture in corotation resonance. The simulation began when occurs the coupling migration between Mimas and Enceladus. In gray a full ring of particles representing possible bodies that may be captured inside the corotation resonance. In last snapshot, we can see all corotations sites which had been captured particles and had been conveyed outward the ring by the interaction with Mimas in its migration process.

mas' eccentricity is in agreement with the results of Meyer & Wisdom (2008). The eccentricity only stops growing when it reaches a certain equilibrium eccentricity (here value is higher 0.052, that was also found by Meyer & Wisdom (2008)) and the satellites escape of Mimas-Enceladus 3:2 e-Mimas resonance. Although we do not show in this work, the eccentricities of Mimas and Enceladus should decrease after they went out of the resonance due to the tidal effects reaching the current values.

These results show that Mimas' eccentricity could be enlarged and hence affect the width of the corotation resonance. In the next section we will study this effect on the capture of particles by the corotation resonance.

5 CAPTURE IN COROTATION RESONANCE

In the previous section we saw that the eccentricity of Mimas increases when Mimas and Enceladus pass through a 3:2 resonance during the tidal migration process. In this section, we will check if this increase in eccentricity will enable Mimas to capture particles in corotation resonance. To perform this study, we created a ring with 10 000 particles in a region where the resonance should appear when the eccentricity of Mimas increase, as we can see in Figure (3a). Thus the particles were uniformly distributed with semi-major axis between 162 409.9 km and 162 604.8 km and with mean longitude between 0° and 360° . All particles have its other orbital elements fixed with the value 0.010 758 38 for eccentricity, $0.004\,053\,321^\circ$ for inclination, 342.0739° for ascending node, and 326.3412° for longitude of the pericenter. These fixed orbital elements were based on the orbital elements of Aegaeon after it was migrated toward Saturn and close to a position where the resonance should appear. This choice was made to improve our chances of capture and we are not interested in finding the best orbital configuration for the capture, but in the migration process as the cause of the capture in corotation resonance.

For this experiment we integrate the full equations of motion for the four body model (Saturn, Mimas, Enceladus and a particle) plus equation (11) acting only in Mimas and

Enceladus and representing the tide interaction in these bodies. We argue that the homogeneous rings do not raise tidal bulges in the planet like moons do, since a homogeneous ring does not raise a tidal bulge. Also, ring's particles have no interaction with each other by collisions or gravity. We also considered an oblate Saturn for all particles involved in the integration. The integrations were made using Gauss-Radau spacings described by Everhart (1985) with initial time step of 0.1 day. We used the same initial conditions for Mimas and Enceladus of table 1. It is important to say that, although all 10 000 particles were integrated at the same time they do not interact with each other. Thus it is a four body problem plus Saturn oblateness for each particle.

In panels (d) and (h) of Figure (3) we can see the evolution of Mimas' eccentricity and in panels (a), (b), (c), (e), (f) and (g) the effects this evolution make in the particles of the ring.

In the very beginning, despite of some small variation, Mimas' eccentricity is not increasing as we can see in Figure (3d). After some time the satellites enter the 3:2 e-Mimas resonance and Mimas' eccentricity increases affecting the ring, as shown in Figure (3b).

In Figure (3c) it is possible to see trapped particles in the resonance which had moved upward due to Mimas migration. In the panels (e), (f) and (g) of Figure (3) we see more explicitly this phenomena where we clearly see six structures moving outside our initial ring. Those six lobes are consistent with a 7:6 corotation resonance. It is also possible to see that some particles were dragged outwards.

To explicitly show that the eccentricity variation is the mechanism responsible for the capture in corotation resonance, we made other experiment passing the corotation resonance through the ring of particles, but with Mimas not varying its eccentricity. For that we take off Enceladus of the simulation and initiate Mimas with its present eccentricity of 0.02 and its semi-major axis 100 km below the value shown in the table (1). For all other orbital elements, it was maintained the values of table (1), and then it was applied the migration process to Mimas. The ring of particles was the same as the last experiment.

We noted that the capture of particles doesn't occur due

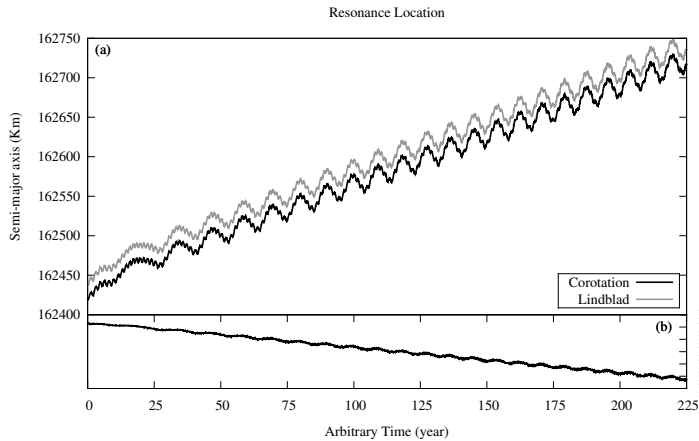


Figure 4. In panel (a) we present the localization of Corotation and Lindblad resonances. These locations were found following the technique of Foryta & Sicardy (1996), with equations of Renner & Sicardy (2006). The Corotation and Lindblad location move because Mimas is migrating during this simulation. In (b) it shows the distance between these resonances.

to overlap between the Lindblad and corotation resonances. These two resonances have a separation about 19 km (Figure 4b) and the particles in the ring trapped by the corotation resonance feel the Lindblad perturbation (El Moutamid, Sicardy & Renner 2014). These simulations show that, in our accelerated tidal scenario, the overlap of resonances isn't the dominant mechanism to capture of particles.

We can see that holes appear while the corotation resonance passes through the ring of particles (see panels (a) to (f) of Figure (5)). As there are no particles inside these holes, we can affirm that particles weren't captured. This effect shows that the corotation resonance cannot capture neither loose particles unless it changes its width. However, we can see that some particles stay close to the corotation edge (Figure (5e)) and Figure (5f)). These particles are temporary captured in a region known as resonance stickiness (Contopoulos & Harsoula 2010). These particles move in the border of the lobes of the corotation resonance for a time and then they escape.

With these results, we show that our scenario could explain the formation of the arc of the G-ring. In this scenario, we used a migration rate much above of that generated by tidal effect, and with a realistic migration rate, it must work as the same way. Actually, we had made our first experiments with rates consistent with tidal migration and observed the robustness of the corotation resonance.

In one of our first experiments, which we have not shown here, we created an arc of 1847 particles in the resonance of Mimas where G ring arc was in date January 1st, 2004 (Hedman et al. 2010), and simulated Mimas migrating with a velocity equal to 9.0×10^{-9} km/year toward Saturn by 1000 years. The final of simulation we found that 98% of the particles was in corotation with Mimas, corroborating the robustness of the corotation resonance.

In this scenario, it was needed a high initial eccentricity for Enceladus to force the escape of Mimas from the 3:2 e-Mimas resonance, but it is not a problem for our scenario because several other processes could take Mimas out of this

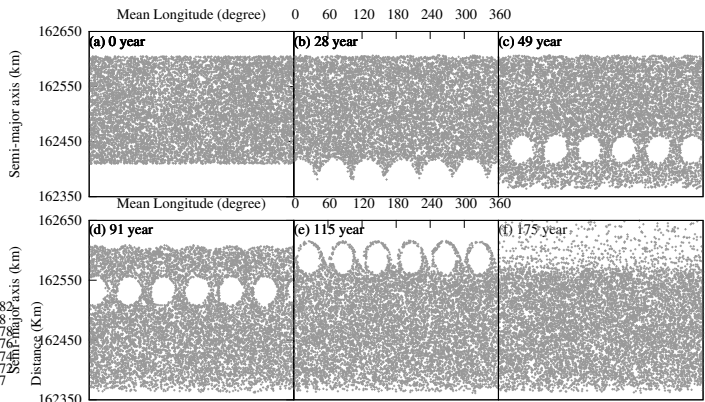


Figure 5. In these six snapshots shown we had taken off Enceladus of the simulation. Without the eccentricity enhancement due to 3:2 resonance there is no capture in the corotation resonance. In last snapshot, all corotation sites have passed through the ring without capture any particle.

resonance, for instance, an eventual resonance between Mimas and Dione.

6 EVOLUTION OF THE CAPTURE RESONANCE

In the last section, we observed that the particles were captured in corotation resonance and dragged out of the ring we created. Now we will analyse these captures through the history of the captures. In Figure (6) we have the ring of particles in time 0 of our simulation and we indicate the particles that were captured. In the Figure (6b), we identified with grey points the particles which were not captured in the Mimas migration process and with black points the particles which were captured in this process and didn't escape the corotation sites during the simulation. The final state of these captured particles (black points in Figure (6b)) can be seen in panel (g) of Figure (3) occupying the corotation sites above the ring of particles.

In the bottom part of the Figure (6b), we saw a draft of the 7:6 corotation sites in its initial condition produced by Mimas eccentricity. The amplitude of the curves obeys the width of the corotation for the initial Mimas eccentricity (equation (5)). With the Mimas migration, the width of this curve will enlarge. This enlargement will produce the captures in the corotation resonances.

We can see in the panel (b) of Figure (6) that the black points are spread in the ring and they show some structures. In panel (a) we show the number of captured particles in bins of 10 km for the semi-major axis. The excess particles in the low part of the disc occur due to Mimas initial eccentricity, as the corotation resonance has an initial width showed by the embedded black points encircled by the draft representing the corotation curves. Observing the structures and the histogram of the graph, it suggests that we hadn't a homogeneous rate of captures. Thus, the capture is not continuous, but in steps. The explanation for that can be obtained ob-

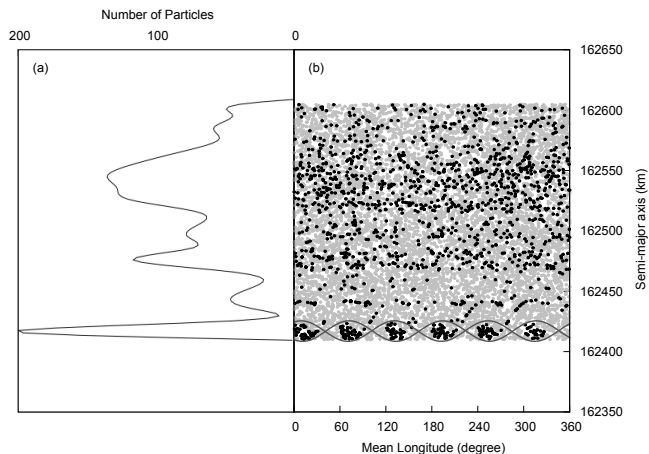


Figure 6. Evolution of the capture in corotation resonance through the ring of particles. Panel (b) of this graph shows the initial conditions of the captured particles. In panel (a) it was shown a histogram of captured particles in ranges of 10 km for the semi-major axis.

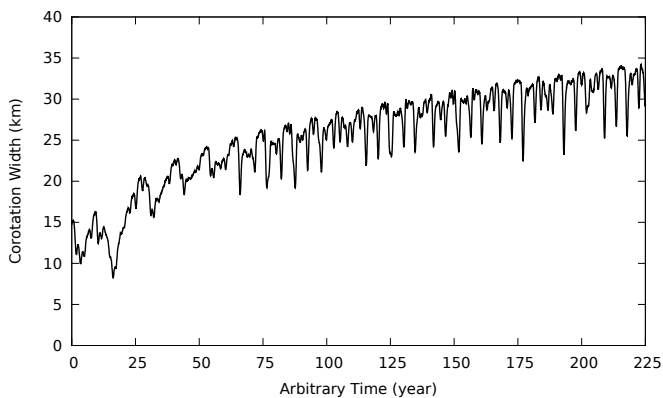


Figure 7. Amplitude evolution of the corotation resonance width based on equation (5) for each value of the Mimas eccentricity of Figure (3).

servicing the graphs of Figure 3 as the eccentricity oscillates while increases.

The capture by the corotation resonance is complex. When Mimas was captured by the 3:2 resonance with Enceladus its eccentricity began to increase but not in a uniform way. In Figure (7) we see the evolution of this width based on equation (5) and the history of Mimas eccentricity shown in Figure (3). The net result of the process double the initial width, however locally it increases and decreases in a very noise form. Thus, particles were captured while there are others that escape from the corotation resonance. The particles that were captured and escaped are the ones in the stickiness caused by the corotation resonance observed in Figure (5). This complex dynamic explains the structures observed in Figure (6).

This feature can be understood when we consider the capture probability in the corotation resonance, which depends on perturbing eccentricity (Quillen 2006), in our case the perturber is Mimas. The Mimas' eccentricity increases non-uniformly (Figure 3), so the capture probability oscil-

lates during the simulation. When the eccentricity increases, it favours the capture, and when it decreases, the escape likelihood increases. The result is a relative capture probability, because sometimes it is more likely to capture particles, but sometimes, it is less likely. It was that which creates the structures observed in Figure (6).

These results lead us to conclude that the migration sweeping over the particles, as shown in Figure (3), with the change in the corotation resonance width producing a change in Mimas' eccentricity, as shown in Figure (6), is the process which could explain the capture of the one particle, or a group of particles, which produced the arc of the G-ring.

7 CONCLUSIONS

In this paper, we showed that it is possible to explain the formation of the arc of the G-ring through a plausible scenario where the Saturn tides play the main role.

The Saturn's tide could vary the semi-major axis of the satellites, which make them cross several resonances. In this process a low Mimas' eccentricity could have increased and could have caused the enlarging of the corotation region.

In our experiment, when Mimas created the region of corotation particles, we had populated all the six structures of the corotation. Then, if there was a ring of particles in the corotation resonance capture region, we should observe other groups today. However, there exists only one arc. Our hypothesis is still plausible, since other effects, such as Poynting-Robertson drag may have destroyed the other groups, or even the region was not as homogeneous as we created them in this scenario. We believe that further studies for the arc of the G-ring formation should solve this problem. Other studies could also answer if the arc was formed by agglomeration or erosion, and all these information together could clarify how and why we have only one group observed in 7:6 corotation resonance.

ACKNOWLEDGMENTS

The authors want to thank Bruno Sicardy for the prolific discussions and helpful suggestions, the anonymous referee for his helpful suggestions, and the Brazilian science funding agencies CAPES, CNPq and FAPESP (grant 2011/08171-3).

REFERENCES

- Burns J. A., Matthews M. S., eds., 1986, *Satellites*. Texas University Press
- Callegari N., Yokoyama T., 2010, *Planet. Space. Sci.*, 58, 1906
- Champanois S., Vienne A., 1999, *Celestial Mechanics and Dynamical Astronomy*, 74, 111
- Contopoulos G., Harsoula M., 2010, *Celestial Mechanics and Dynamical Astronomy*, 107, 77
- Cooper N. J., Murray C. D., Evans M. W., Beurle K., Jacobson R. A., Porco C. C., 2008, *Icarus*, 195, 765
- El Moutamid M., Sicardy B., Renner S., 2014, *Celestial Mechanics and Dynamical Astronomy*, 118, 235
- Everhart E., 1985, 185
- Foryta D. W., Sicardy B., 1996, *Icarus*, 123, 129

- Hedman M. M. et al., 2007, *Science*, 317, 653
Hedman M. M., Cooper N. J., Murray C. D., Beurle K., Evans M. W., Tiscareno M. S., Burns J. A., 2010, *Icarus*, 207, 433
Hedman M. M., Murray C. D., Cooper N. J., Tiscareno M. S., Beurle K., Evans M. W., Burns J. A., 2009, *Icarus*, 199, 378
Lainey V. et al., 2012, *ApJ*, 752, 14
Meyer J., Wisdom J., 2007, *Icarus*, 188, 535
Meyer J., Wisdom J., 2008, *Icarus*, 193, 213
Murray C. D., Dermott S. F., 1999, *Solar System Dynamics*. Cambridge University Press
Poulet F., Sicardy B., 2001, *Monthly Notices of Royal Astronomical Society*, 322, 343
Quillen A. C., 2006, *Monthly Notices of Royal Astronomical Society*, 365, 1367
Renner S., Sicardy B., 2006, *Celestial Mechanics and Dynamical Astronomy*, 94, 237
Spitale J. N., Jacobson R. A., Porco C. C., Owen, Jr. W. M., 2006, *AJ*, 132, 692

APPENDIX A:

Poulet & Sicardy (2001) affirm that the attraction of the tidal bulge raised on a planet by a satellite outside the synchronous orbit results in a gain of angular momentum by the satellite. This causes the orbit of the satellite to expand and the rate of change of its semi-major axis is

$$\frac{\dot{a}}{a} = 3 \left(\frac{G}{M_p} \right)^{1/2} k_{2p} \frac{R_p^5}{Q_p} \frac{m}{a^{13/2}}, \quad (\text{A1})$$

where the parameters a , \dot{a} , m , are the semi-major axis, its variation and the mass of the satellite, whereas G is the gravitational constant, M_p is the mass of the planet, k_{2p} is the Love number of the planet and Q_p is the dissipation factor.

We consider that the semi-major axis of Mimas and Enceladus suffered changes described by Equation (A1). If we integrate this equation, keeping M_p , k_{2p} and Q_p constant over time and using parameters of Mimas and Enceladus, we can find the values of semi-major axis for Mimas which enables its trapping with Enceladus into a resonance in the remote past.

The first consideration is that the physical properties of the planet are constant, so we can write that

$$\xi = 3 \left(\frac{G}{M_p} \right)^{1/2} k_{2p} \frac{R_p^5}{Q_p}, \quad (\text{A2})$$

where ξ is a constant depending on the planet parameters. Consequently, the equation (A1) becomes

$$\dot{a} = a^{-11/2} \xi m. \quad (\text{A3})$$

And integrating it we have

$$\frac{2}{13} \left(a^{13/2} - a_0^{13/2} \right) = \Delta t \xi m. \quad (\text{A4})$$

where the integral constant a_0 is the value of semi-major axis at t_0 , and $\Delta t = t - t_0$. Calculating the value of this integral with the parameters of Mimas, we have

$$\frac{2}{13} \left(a_M^{13/2} - a_{0M}^{13/2} \right) = \Delta t_M \xi m_M, \quad (\text{A5})$$

where a_M and a_{0M} are the current and ancient semi-major axis of Mimas, respectively, m_M is Mimas' mass and Δt_M is the time spent for Mimas to vary its position from a_{0M} to a_M .

Using that integral with parameters of Enceladus, we get

$$\frac{2}{13} \left(a_E^{13/2} - a_{0E}^{13/2} \right) = \Delta t_E \xi m_E, \quad (\text{A6})$$

where M was replaced with E .

Now, if we consider that t is the current time and t_0 is an instant that these satellites would be in resonance we have $\Delta t_M = \Delta t_E$, and also the semi-major axes rate of Mimas and Enceladus for the resonance is $\alpha = a_{0M}/a_{0E}$. Then, from equations (A5) and (A6), we find that

$$a_{0M} = \left[\frac{\left(\frac{m_E}{m_M} \right) a_M^{13/2} - a_E^{13/2}}{\left(\frac{m_E}{m_M} \right) - \frac{1}{\alpha^{13/2}}} \right]^{2/13}. \quad (\text{A7})$$

Therefore, with equation (A7) we calculate an approximate value for the ancient semi-major axis of Mimas, just when that satellite was trapped in resonance with Enceladus, given an appropriate α .

This paper has been typeset from a $\text{T}_{\text{E}}\text{X}/\text{L}^{\text{A}}\text{T}_{\text{E}}\text{X}$ file prepared by the author.